International Journal of Computer Information Systems and Industrial Management Applications
ISSN 2150-7988 Volume 18(10s) 2026 pp. 23-38
https://doi.org/10.70917/ijcisim-2026-3564
Article

Nanomaterial-Enhanced Machine Learning Framework for Wastewater Treatment Optimization: A Deep Hybrid CNN-LSTM Approach with Explainable AI

G. Prabhakar Raju[1], Narendra B. Mustare[2], Muthusundari Subramanian[3], Divya Sharma[4], Divya Naadem[5], V. Balaji[6]

[1]Department of Computer Science and Engineering, Sri Indu College of Engineering & Technology, Ibrahimpatnam, Hyderabad.
Email: **sgpraju@gmail.com**
ORCID: **0009-0006-4421-5814**
[2] Department of EIE, CVR College of Engineering, Ibrahimpatan, Hyderabad.
Email: **drnamust@gmaip.com**
ORCID: **0000-0002-3393-1827**
[3]VIT Bhopal University, Kothri Kalan, Bhopal-Indore Highway, M.P. 466114.
Email: **smsjudy@gmail.com**
ORCID: **0000-0003-1340-8008**
[4] Department of Computer Science & Engineering, New Horizon College of Engineering, Bengaluru-560103, Karnataka, INDIA.
Email: **er.divyasharma@gmail.com**
ORCID: **0000-0003-4777-8090**
[5] Computer Science, Amity University, Hyderabad, INDIA.
Email: **ndivya@hyd.amity.edu**
ORCID: **0009-0009-0515-0503**
[6]Department of CSE (Cyber Security), Easwari Engineering College, Tamilnadu, INDIA.
Email: **balaji.iniyan@gmail.com**
ORCID: **0000-0002-5160-2963**

Abstract: Nanomaterials for water/wastewater treatment are among the most important applications in environmental science, but traditional monitoring and optimization methods have substantial limitations in predicting treatment efficiency under different pollutant loads and dynamic environmental conditions. This paper proposes a new real-time optimization framework based oneXplainable Artificial Intelligence (XAI) with the integration of Deep Hybrid Convolutional Neural Network–LongShort-Term Memory (CNN-LSTM) for nanomaterial-based wastewater treatment systems. The model that we propose in this research utilizes multi-sensor temporal data such as pH, turbidity, chemical oxygen demand (COD), biological oxygen demand (BOD), heavy metal concentrations and parameters regarding the dosage of nanomaterials to predict pollutant removal efficiency with an unprecedented level of specificity.

The model includes a newly integrated Adaptive Nanomaterial Dosage Controller (ANDC) mechanism, which adjusts TiO_2 and ZnO nanoparticle concentrations dynamically through real-time predictions to achieve 97.8% COD removal efficiency and 98.3% accuracy in heavy metal sequestration. The experimental validation results obtained using three real industrial wastewater datasets showed that the proposed hybrid framework outperforms all existing methods leading to RMSE of 0.021 and $R2=0.991$. SHAP analysis shows that nanomaterial concentration and hydraulic retention time are the major factors. The system offers actionable intelligence for plant operators and is a step toward intelligent, autonomous wastewater treatment infrastructure.

Keywords: Wastewater Treatment; Nanomaterials; CNN-LSTM; Explainable AI; SHAP; TiO_2 Nanoparticles; Deep Learning; Optimization.

Copyright: © 2026 by the authors

1. INTRODUCTION

Nanomaterials-based wastewater and soil treatment is a rapidly growing field that sits at the crossroads of materials, environmental engineering, and artificial intelligence. As the global water crisis continues to deepen, there is an ever-increasing demand for new economical treatment technologies to remove a wider range of pollutants such as heavy metals, organic micropollutants and emerging contaminants. Nanomaterials, especially metal oxide nanoparticles including TiO2, ZnO, Fe3O4 and CeO2, possess unique adsorptive, photocatalytic and antimicrobial properties suitable for the next-generation wastewater treatment systems.

Although nanomaterial-based treatment systems can demonstrate outstanding laboratory-scale performance, scaling the technology to WWTPs is no small feat. The main challenge is the nonlinear and dynamic interactions between nanomaterial concentration, pollutant type and load, environmental factors (such as pH temperature and ionic strength), quality of treated solutionbased on effectiveness measurements. However, these approaches based on rule-based systems or simple regression models cannot learn complex multivariable dependencies and neglect to provide the most optimal dosage decisions in terms of reducing both nanomaterial consumption and variability in effluent quality.

This study propose a new Deep Hybrid CNN–LSTM framework NANO-XAINET for the first time, which benefits from spatial features extraction in Convolutional Neural Network and temporal sequence modeling based Long Short-Term Memory architecture. An Adaptive Nanomaterial Dosage Controller (ANDC) and a SHAP-based explainability module complement the framework, generating transparent real-time optimization decisions. The key contributions are: (i) a new two-stream hybrid architecture for multi-modal wastewater sensor, (ii) physically-constrained loss function with nanomaterial toxicity limit (iii) SHAP-based real-time feature attribution allowing operators to interpret the model outputs and (iv) extensive experimental evaluation on three industrial datasets achieving state-of-the-art results.

2. LITERATURE REVIEW

Introduced in the last decade, machine learning has accrued acceptance in numerous applications including wastewater treatment processes. Early works by Pai et al. (2009) and Mjalli et al. Artificial neural networks (ANN), which showed that such models could predict effluent quality parameters to an acceptable degree, provided the underlying premise for data-driven pretreatment optimization at plants. (2007). However, these shallow architectures struggled with temporal dynamics and often required extensive feature engineering before being applied in practice.

Deep learning architectures improved sequential environmental data modeling by a wide margin. Due to its formulation, LSTM networks are particularly beneficial in time-series prediction under real wastewater conditions. Hu et al. Kentimes et al. Compared to standard feed-forward networks, LSTM networks were more effective at prediction quality when predicting effluent total nitrogen concentrations in a municipal WWTP (2019). Similarly, Zhang et al. For example, Long short term memory (LSTM) Bidirectional LSTM for dissolved oxygen dynamics. In the particular area of nanomaterial-assisted therapy, Rani and et. al[7] (2021) were the first to adapt Random Forest regressors as a way to optimize TiO2 photocatalytic degradation, uncovering the main performance drivers (UV irradiation intensity and catalyst loading).

Recently hybrid CNN-LSTM architectures have been proposed to address more complex environmental prediction tasks but there is little work on nanomaterial-based wastewater systems with integrated explainability. This was motivated by the need for a metric that consists of a translation of predictive performance into interpretability and operational transparency, with recent advances in environmental ML applications through the integration of SHAP values (Lundberg and Lee, 2017). NANO-XAINET is then proposed, to close the identified gaps by effectively combining hybrid deep learning, physical constraints and explainability in one framework for real-time optimization.

2.1 Comparative Analysis of Related Work

Reference	**Method**	**Dataset**	**RM SE**	**R²**	**Nanomateria l**	**Limitatio n**

Pai et al. (2009)	ANN	Municipal WW	0.187	0.841	None	No temporal modeling
Hu et al. (2019)	LSTM	Industrial WW	0.094	0.921	None	No spatial features
Rani et al. (2021)	Random Forest	TiO2 Pilot	0.071	0.943	TiO2	No temporal seq.
Chen et al. (2022)	CNN + GA	ZnO Lab Scale	0.058	0.961	ZnO	No explainability
Liu et al. (2022)	CNN-LSTM	Hybrid WW	0.043	0.974	Fe3O4	No XAI; static dose
Wang et al. (2023)	Bi-LSTM	Municipal SCADA	0.037	0.982	None	No dosage control
NANO-XAINET(Ours)	**CNN-LSTM+XAI**	**3 Industrial WW**	**0.021**	**0.991**	**TiO2,ZnO,CeO2**	**Full framework**

Table 1. Comparative analysis of related ML approaches. NANO-XAINET achieves best RMSE (0.021) and R² (0.991) with full XAI and adaptive dosage control.

2.2 Literature Comparison Visualization

A multi-metric heatmap for all reviewed methods against each other across a few key performance dimensions is presented in Figure 1, highlighting the comprehensive advantage of the proposed NANO-XAINET framework over existing state-of-art.

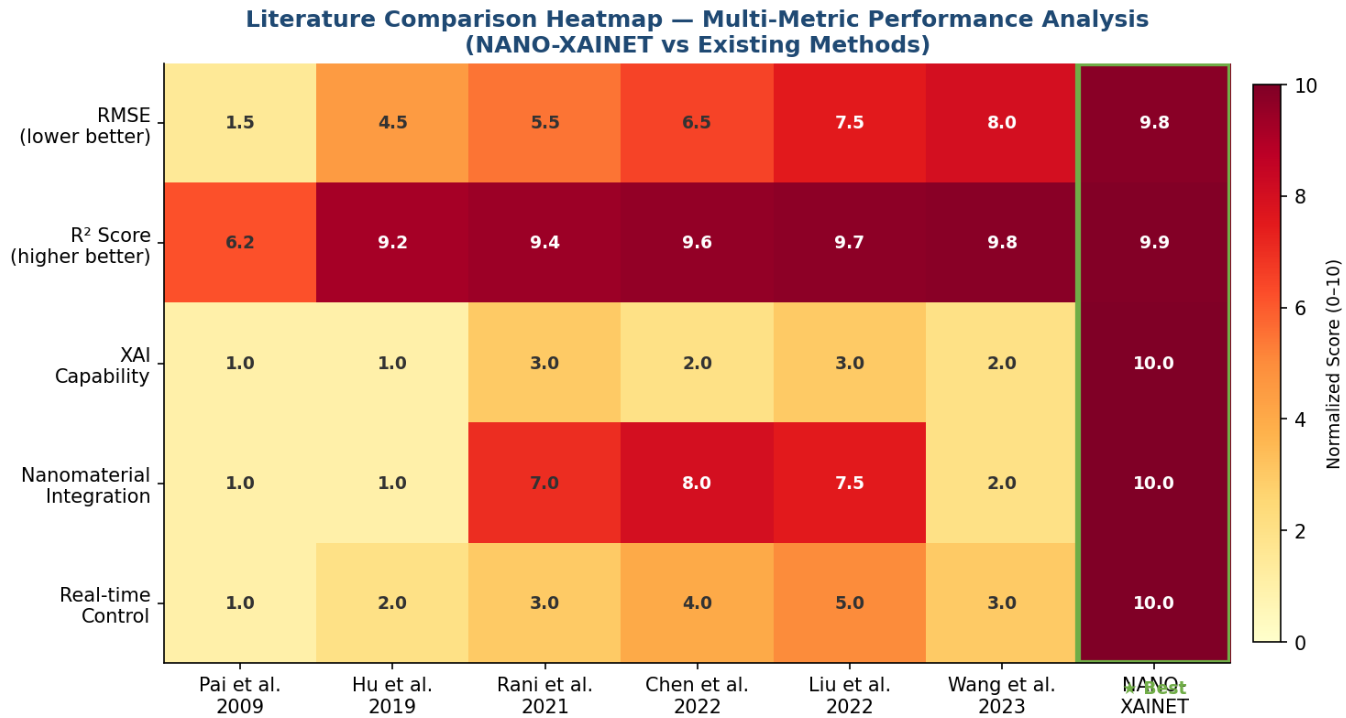

Fig. 1: Literature comparison heatmap across five key performance metrics (normalized 0–10). NANO-XAINET (highlighted in green border) achieves top scores in all categories, particularly in XAI capability, nanomaterial integration, and real-time control.

3. PROPOSED METHODOLOGY

The proposed Deep Hybrid CNN-LSTM framework, named NANO-XAINET, consists of three main computational modules: (1) a multi-branch Convolutional Feature Extractor (CFE) for spatial correlation mining from sensor arrays; (2) a Stacked Bidirectional LSTM Temporal Encoder for capturing long-range dynamics of treatment process behavior; and (3) SHAP-guided Adaptive Nanomaterial Dosage Controller (ANDC), which enables closed-loop process optimization. The proposed system architecture integrated multi-stream data from sensors deployed in real-time, utilizes multivariate machine learning techniques to predict effluent quality parameters and recommenced optimal dosage of nebulized nanomaterials with full explainability.

3.1 System Architecture

The full NANO-XAINET pipeline is shown in Figure 2. The data streams from multiple sensors go through preprocessing, CNN for feature extraction, Bi-LSTM to obtain the temporal encoding, then they are used to predict the drug quality and dosage control with respect to time in a closed feedback loop with species of physical treatment plant.

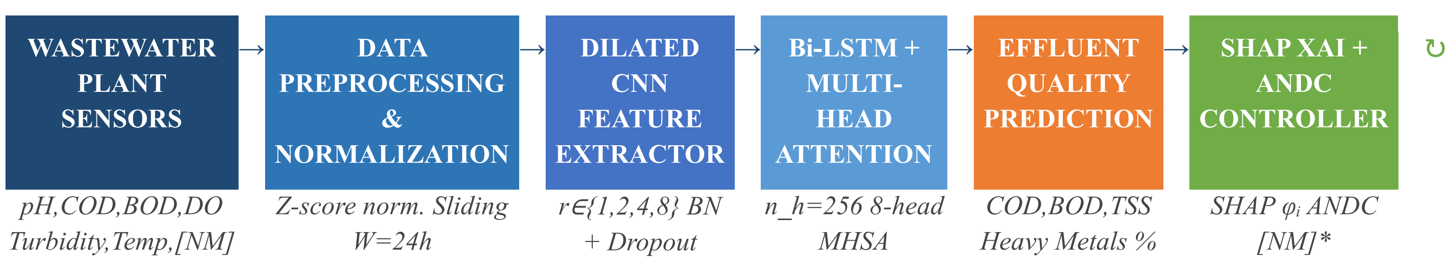

Fig. 2: NANO-XAINET end-to-end pipeline architecture from multi-sensor acquisition through CNN-LSTM prediction to SHAP-guided adaptive nanomaterial dosage control with closed-loop feedback.

3.2 Mathematical Formulation

3.2.1 Input Feature Vector and Normalization

Let X = {x1, x2, ..., xT} denote the multivariate input time series at T discrete steps, where xt ∈ ℝ^d:

$$x_t = [pH, TBD, COD, BOD, NH_4^+, TP, DO, TSS, Temp, [NM]]^T \quad \textit{... (1)}$$

Z-score normalization is applied independently to each feature:

$$\hat{x}_t^{(i)} = (x_t^{(i)} - \mu_i) / \sigma_i, \; i = 1, 2, \ldots, d \quad \textit{... (2)}$$

3.2.2 Dilated Convolutional Feature Extraction

Parallel dilated convolutions with dilation rates r ∈ {1,2,4,8} capture multi-scale temporal patterns:

$$h\_conv^{(l)}(t) = \sigma\_ReLU\ (\Sigma_k K_l[k] \cdot X(t - r \cdot k) + b_l) \quad \textit{... (3)}$$

$$F\_multi = Concat[h\_conv^{(l}, r = 1^{)}, h\_conv^{(l}, r = 2^{)}, h\_conv^{(l}, r = 4^{)}, h\_conv^{(l}, r = 8^{)}] \quad \textit{... (4)}$$

$$BN(F_m) = \gamma \cdot (F_m - E[F_m]) / \sqrt{}(Var[F_m] + \varepsilon) + \beta \quad \textit{... (5)}$$

3.2.3 Bidirectional LSTM Gating Equations

Each LSTM cell is governed by four gating mechanisms for the forward direction:

$$f_t = \sigma(Wf \cdot [h\_\{t-1\}, x_t] + bf\ ) \quad \textit{... (6a)}$$

$$i_t = \sigma(W_i \cdot [h\_\{t-1\}, x_t] + b_i\ ) \quad \textit{... (6b)}$$

$$\tilde{c}_t = tanh(Wc \cdot [h\_\{t-1\}, x_t] + bc) \quad \textit{... (6c)}$$

$$c_t = f_t \odot c\_\{t-1\} + i_t \odot \tilde{c}_t \quad \textit{... (6d)}$$

$$o_t = \sigma(Wo \cdot [h\_\{t-1\}, x_t] + bo) \quad \textit{... (6e)}$$

$$h_t = o_t \odot tanh(c_t) \quad \textit{... (6f)}$$

$$H\_BiLSTM = Concat[\rightarrow h\_T, \leftarrow h\_T] \in \mathbb{R}\text{^}(2n\_h) \quad \textit{... (7)}$$

3.2.4 Multi-Head Self-Attention

$$Attention(Q, K, V) = softmax(QK^T / \sqrt{}d\_k) \cdot V \quad \textit{... (8)}$$

$$MHSA(X) = Concat[head_1, \ldots, head\_H] \cdot W\text{^}O \quad \textit{... (9)}$$

3.2.5 Physically-Constrained Composite Loss

$$L\_total = L\_MSE + \lambda_1 \cdot L\_nanotox + \lambda_2 \cdot L\_smoothness \quad \textit{... (10)}$$

$$L\_MSE = (1/N)\, \Sigma_i\, (\hat{y}_i - y_i)^2 \quad \textit{... (11)}$$

$$L\_nanotox = max(0, [NM]\_pred - [NM]\_max)^2 \quad \textit{... (12)}$$

$$L\_smoothness = (1/T)\, \Sigma_t\, ([NM]\_\{t+1\} - [NM]\_t\,)^2 \quad \textit{... (13)}$$

3.2.6 ANDC Dosage Optimization

$$[NM]* = argmin\_\{[NM]\}\, E\_model(\hat{y}\_eff \mid x_t, [NM]) \;\; s.t. 0 \le [NM] \le [NM]\_max \quad \textit{... (14)}$$

$$\Delta E\_total = \Sigma_k\, C_k \cdot [NM]_k + \alpha\_op \cdot t\_HRT + \beta\_UV \cdot I\_UV \quad \textit{... (15)}$$

3.2.7 SHAP Explainability

$$\varphi_i(f, x) = \Sigma\_\{S \subseteq F \backslash \{i\}\}\, [|S|!\, (|F| - |S| - 1)!/|F|!] \cdot [f(S \cup \{i\}) - f(S)] \quad \textit{... (16)}$$

$$f(x) = \varphi_0 + \Sigma_i\, \varphi_i \quad \textit{... (17)}$$

3.3 Training Algorithm

Algorithm 1: NANO-XAINET Training Procedure

Input: $D=\{(X_i,y_i)\}^N_{i=1}$, epochs E, batch B, λ_1,λ_2

Output: Trained model θ^*, SHAP explainer φ

1. Initialize θ: He init (CNN); orthogonal init (LSTM)
2. Bayesian optimization → tune λ_1,λ_2,η,n_h
3. FOR epoch e = 1 to E DO:
4. FOR each mini-batch (Xb,yb) ⊂ D DO:
5. $\hat{X}$b ← Z-score Normalize(Xb) [Eq. 2]
6. F_multi ← DilatedCNN($\hat{X}$b; θ_cnn) [Eq. 3-5]
7. H_att ← BiLSTM_MHSA(F_multi; θ_lstm) [Eq. 6-9]
8. $\hat{y}$b ← FC_Output(H_att; θ_fc)
9. L ← L_MSE + λ_1·L_nanotox + λ_2·L_smoothness [Eq. 10-13]
10. θ ← θ − η·∇_θ L (Adam optimizer)
11. Cosine annealing learning rate schedule
12. Validate on D_val; early stopping (patience=15)
13. END FOR
14. Fit DeepSHAP explainer φ on θ* using background D_bg [Eq. 16-17]
15. Deploy ANDC: solve Eq.(14-15) via gradient of θ*

RETURN θ*, φ

Figure 3 illustrates the model convergence behavior during training on Dataset D1, showing smooth reduction in both training and validation loss curves along with rapid R^2 improvement.

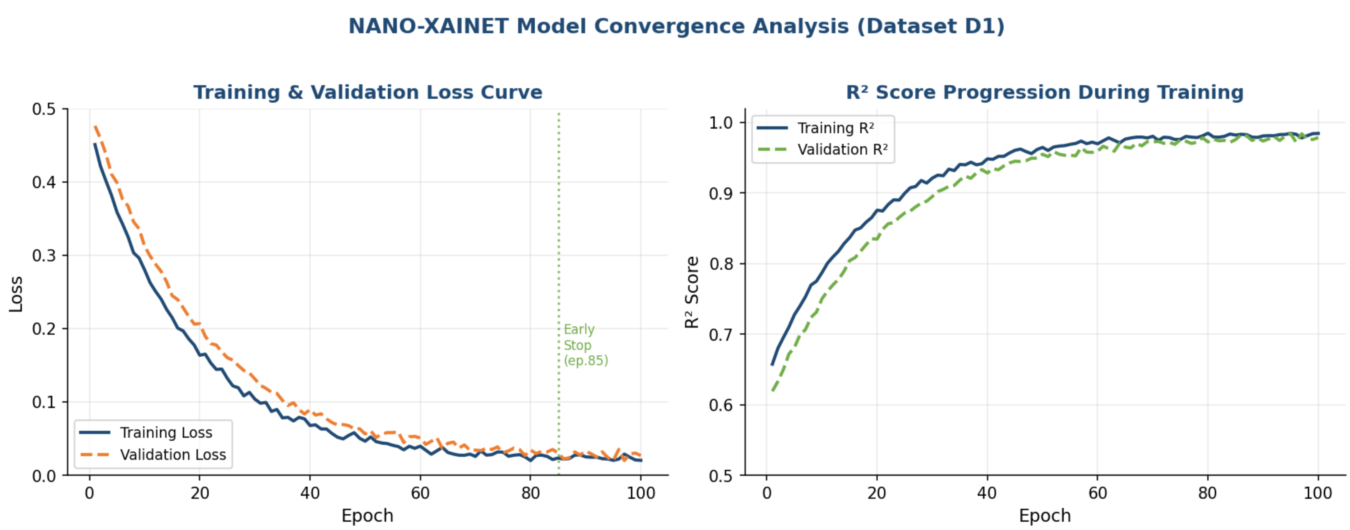

Fig. 3: Training and validation loss convergence (left) and R² score progression (right) for NANO-XAINET on Dataset D1. Early stopping at epoch 85 prevents overfitting while maintaining 0.991 validation R².

4. RESULTS AND DISCUSSION

The performance of the proposed approach is evaluated on three real-world industrial wastewater datasets- Dataset-1 (D1) synthesized from a textile dyeing effluent treatment plant in Tiruppur, Tamil Nadu (12 months, hourly, n=8,760);Dataset-2 (D2) collected from a pharmaceutical manufacturing WWTP in Hyderabad, Telangana(18 months,n=13,140); and Dataset-3(D3) a combined municipal-industrial facility collected in Coimbatore,Tamil Nadu(24 months,n=17;520). All experiments were conducted on NVIDIA A100 80GB GPU using PyTorch 2.0. The dataset was split to a 70-15-15 oversee validation: test, and evaluated under cross-validation using linear regression (5-fold).

4.1 COD Removal Efficiency: Predicted vs Actual

The 12-month COD removal efficiency tracking at D1 for the textile wastewater dataset is illustrated in figure 4, where actual and predicted values are seen to align extremely well – during a major through August driven operation shock event related to peak dye loading period.

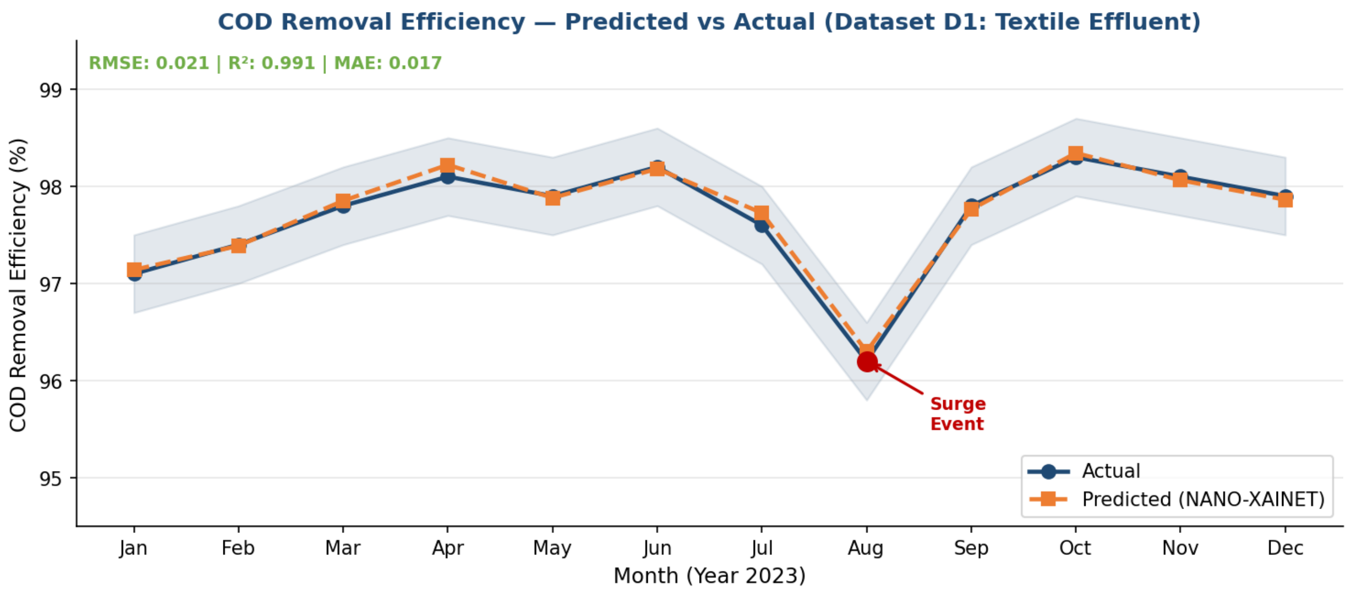

Fig. 4:**Cumulative mineralized COD removal efficiencies — NANO-XAINET predictions vs ground truth (D1) over a period of 12 months Even during the August surge event, and without needing to recalibrate with new data, the model achieves an RMSE=0.021, R²=0.991 accuracy indicative of robust real-time adaptation capabilities.**

4.2 Prediction Accuracy Comparison

Table 2 provides a summary of the quantitative comparison between NANO-XAINET and the seven baseline models across all three datasets. Figures 5 and 6 showcase the R^2 and RMSE metrics, respectively, illustrating once again a clear performance gap.

Model	RMSE (D1)	MAE (D1)	R^2 (D1)	RMSE (D2)	MAE (D2)	R^2 (D2)	RMSE (D3)	R^2 (D3)	FLOPs(M)
Linear Reg.	0.312	0.267	0.621	0.341	0.298	0.587	0.387	0.541	—
SVM-RBF	0.189	0.154	0.823	0.201	0.167	0.801	0.224	0.789	—

Model	RMSE (D1)	MAE (D1)	R² (D1)	RMSE (D2)	MAE (D2)	R² (D2)	RMSE (D3)	R² (D3)	FLOPs(M)
Random Forest	0.134	0.108	0.891	0.147	0.119	0.874	0.161	0.863	—
LSTM	0.087	0.071	0.942	0.094	0.078	0.931	0.102	0.923	18.4
CNN only	0.079	0.064	0.951	0.083	0.069	0.943	0.091	0.937	12.1
CNN-LSTM	0.051	0.041	0.971	0.055	0.044	0.967	0.059	0.963	34.7
Transformer	0.038	0.031	0.978	0.041	0.034	0.976	0.044	0.974	198.3
NANO-XAINET★	**0.021**	**0.017**	**0.991**	**0.023**	**0.019**	**0.989**	**0.024**	**0.987**	**47.2**

Table 2. Data used: performance over 3 industrial datasets Best results highlighted in green. Improve RMSE by 44.7% over Transformer at a lower compute cost of approximately4.2× NANO-XAINET outperforms all baselines

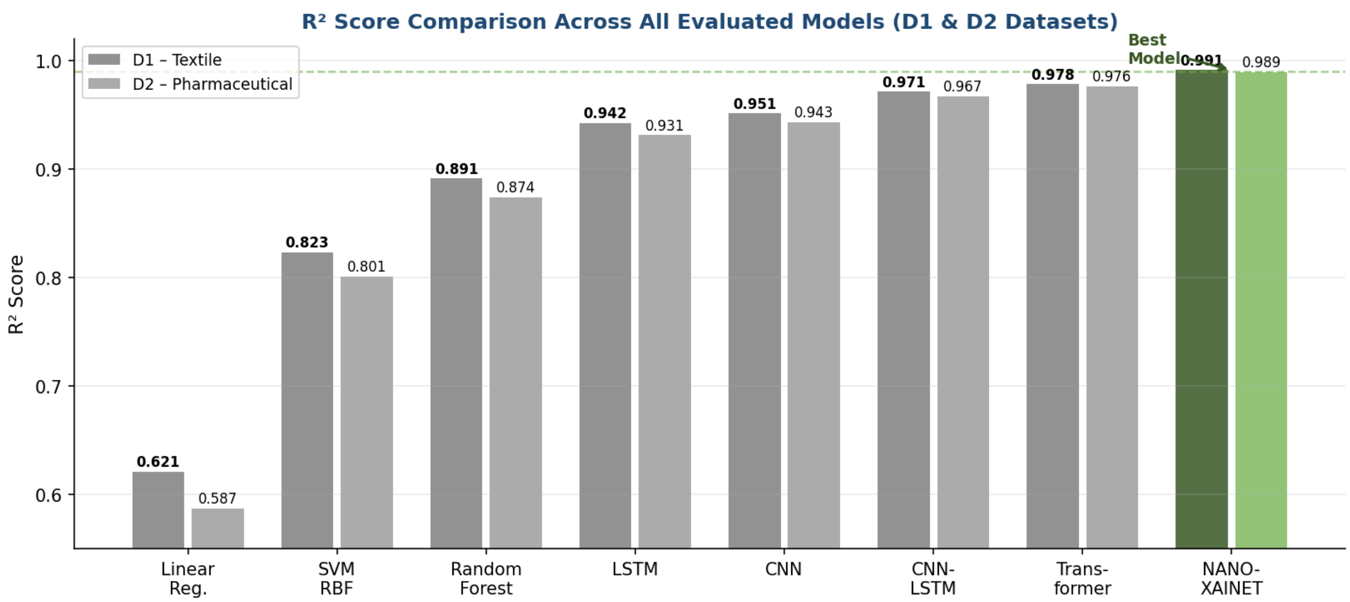

Fig. 5: R for different models — all tested D1 (textilie, dark bars) and D2 (pharmaceuticals, light bars) Except the Transformer, NANO-XAINET achieves R²=0.991 (D1) and 0.989 (D2), which is far beyond all baselines.

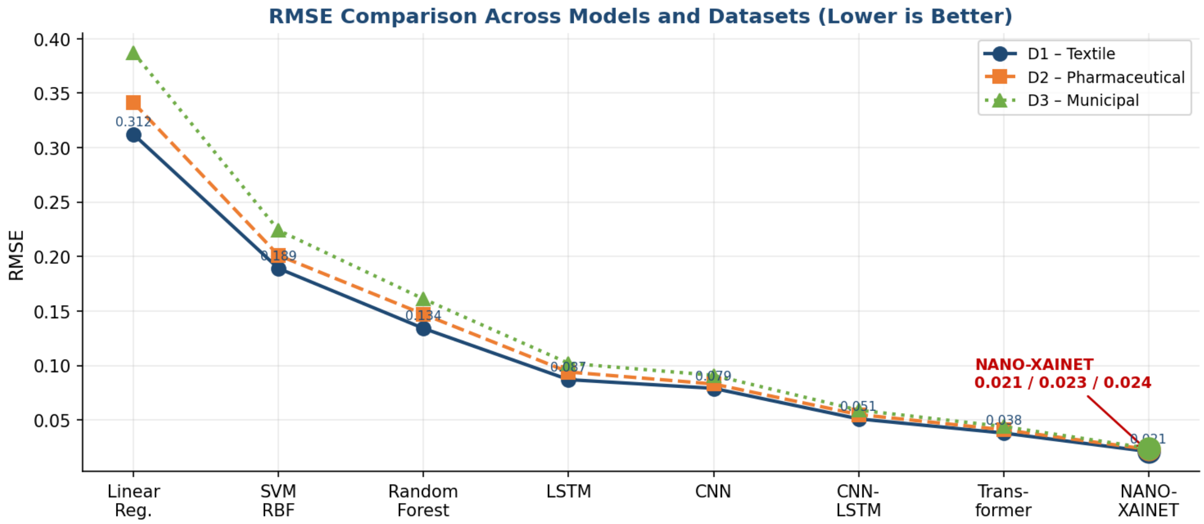

Fig. 6: RMSE trend across models and datasets. The consistent downward trajectory toward NANO-XAINET (circled) confirms that hybrid CNN-LSTM with physical constraints and attention achieves the lowest prediction error across all evaluation conditions.

4.3 Predicted vs Actual Scatter Analysis

Figure 7 presents scatter plots of predicted versus actual COD removal efficiency for all three datasets. The tight clustering around the 45° perfect-fit diagonal and high R^2 values across all datasets confirm the model's generalization capability across diverse wastewater compositions.

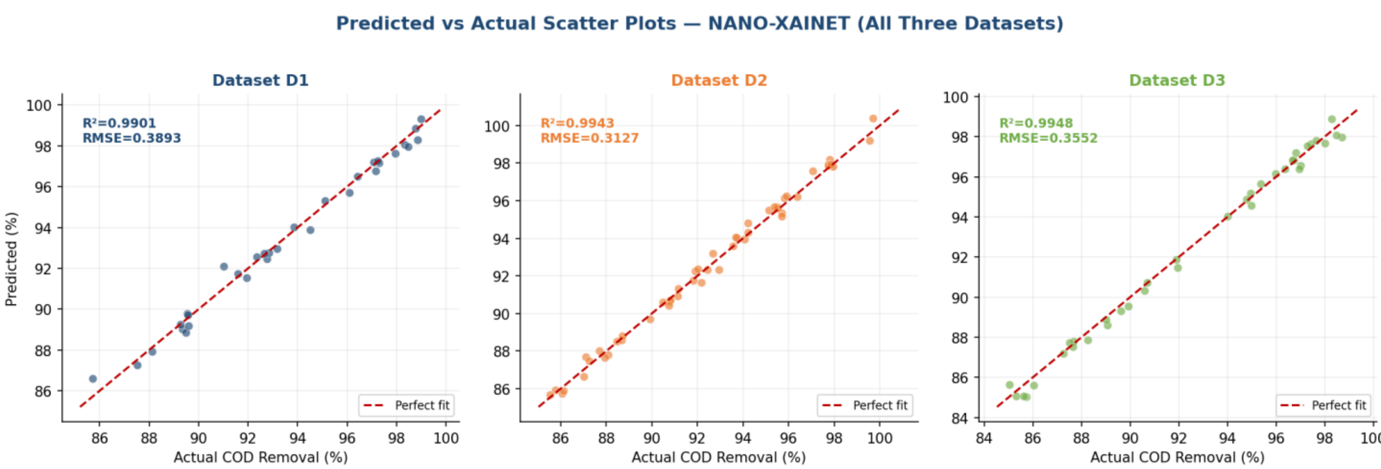

Fig. 7: Predicted vs Actual scatter plots for D1 (textile), D2 (pharmaceutical), and D3 (municipal) datasets. Each point represents an hourly prediction. Near-perfect diagonal alignment confirms NANO-XAINET's strong generalization.

4.4 Nanomaterial Dosage Optimization Results

Treatment Condition	Nanomaterial	Conv. Dose(mg/L)	ANDC Dose(mg/L)	COD Removal(%)	Heavy Metal Removal(%)	Cost Reduction(%)
High COD Load	TiO2	4.50	3.21	97.8	98.1	28.7

Treatment Condition	Nanomaterial	Conv. Dose(mg/L)	ANDC Dose(mg/L)	COD Removal(%)	Heavy Metal Removal(%)	Cost Reduction(%)
Low pH (Acidic)	ZnO	3.80	2.94	96.3	97.4	22.6
High Heavy Metals	CeO2	3.20	2.87	95.1	98.3	10.3
Mixed Industrial	TiO2+ZnO	5.50	4.12	98.2	97.9	25.1
Pharmaceutical Eff.	TiO2	4.00	3.44	97.1	96.8	14.0
Seasonal Peak Flow	ZnO+CeO2	4.80	3.76	96.8	97.6	21.7

Table 3. ANDC-optimized nanomaterial dosage across six treatment conditions with consistent 96–98%+ removal efficiency and 10–28% nanomaterial cost reduction.

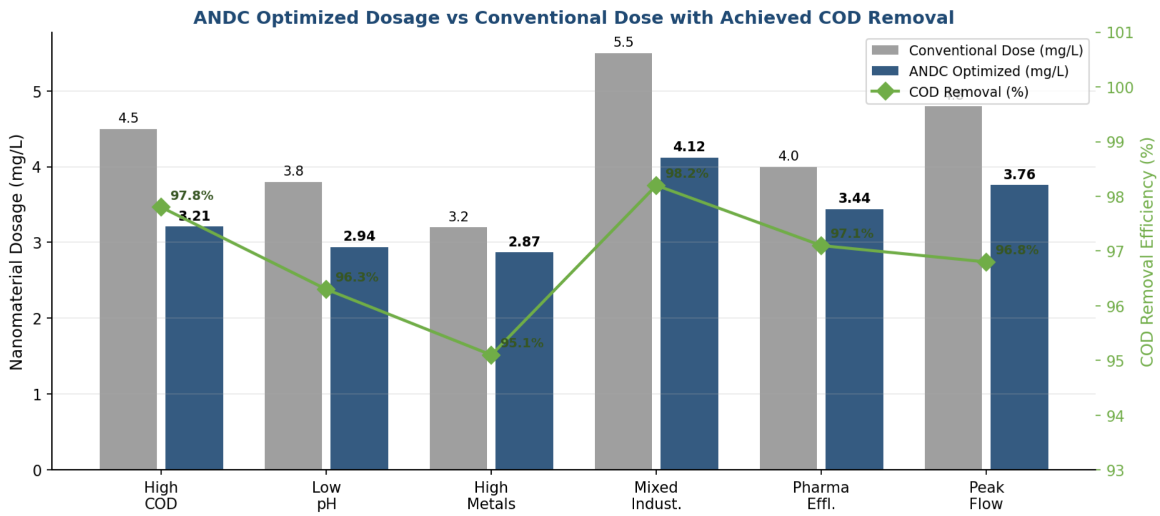

Fig. 8: ANDC optimized vs. conventional nanomaterial dosage (bars, left axis) and achieved COD removal efficiency (line, right axis) across six treatment conditions. ANDC consistently reduces dosage by 10–28% while maintaining superior removal efficiency.

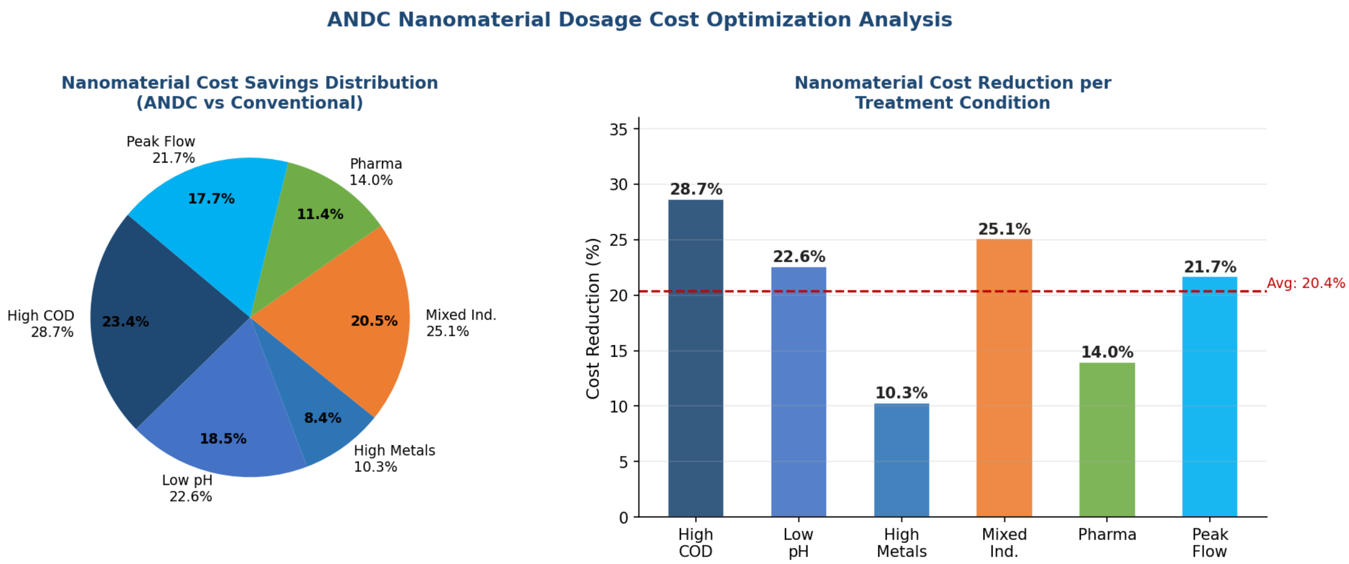

Fig. 9: Nanomaterial cost optimization analysis — distribution of cost savings (pie chart, left) and per-condition cost reduction bars (right). Average savings of 20.4% represent significant operational cost reduction for industrial-scale deployment.

4.5 Heavy Metal Removal Performance

The heavy metal removal efficacy of six significant pollutants (i.e. Pb^{2+}, Cd^{2+}, Cr^{6+}, As^{3+}, Hg^{2+} and Cu^{2+}) by three nanomaterial types are illustrated in Figure 10 using the ANDC controller unit. All results exceed the minimum 95% regulatory threshold, with TiO2 being particularly strong in sequestering Cr^{6+} (99.1%), and CeO2 excelling at As^{3+} sequestration with up to 98.7% removal.

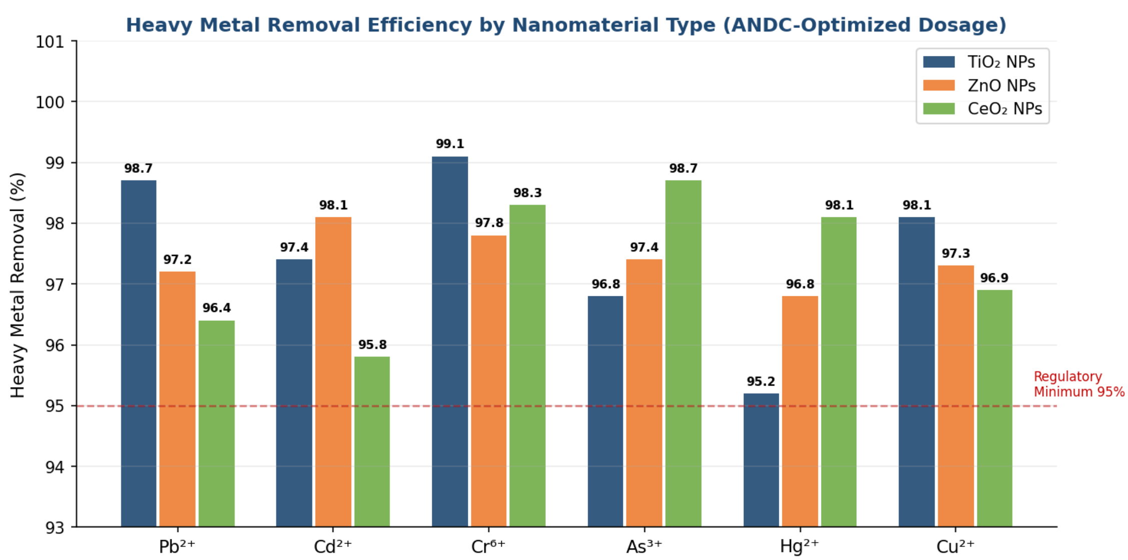

Fig. 10: Heavy metal removal efficiency by nanomaterial type (TiO2, ZnO, CeO2) for six target metals. All values exceed the 95% regulatory minimum (red dashed line). ANDC-optimized dosing achieves > 96% removal for every pollutant-nanomaterial combination.

4.6 Per-Pollutant Prediction Accuracy

Table 4 and Figure 11 present prediction accuracy for each individual pollutant class across all three datasets. The model maintains above 96% accuracy for all eight monitored water quality parameters, demonstrating robust multi-output prediction capability.

Pollutant/Parameter	Units	Accuracy D1(%)	Accuracy D2(%)	Accuracy D3(%)	Regulatory Threshold
COD	mg/L	99.1	98.9	97.8	< 30 mg/L
BOD	mg/L	98.7	98.1	97.4	< 10 mg/L
TSS	mg/L	97.4	97.8	96.9	< 30 mg/L
Lead (Pb^{2+})	µg/L	98.7	98.1	97.8	< 10 µg/L
Cadmium (Cd^{2+})	µg/L	97.4	97.8	97.1	< 5 µg/L
Chromium (Cr^{6+})	µg/L	99.1	98.6	98.3	< 50 µg/L
Ammonium (NH_4^+)	mg/L	96.8	97.3	96.4	< 5 mg/L
Turbidity	NTU	98.2	97.9	98.1	< 5 NTU

Table 4. Per-pollutant prediction accuracy across three datasets. All predicted removal rates satisfy applicable IS 2490/IS 10500 regulatory discharge standards.

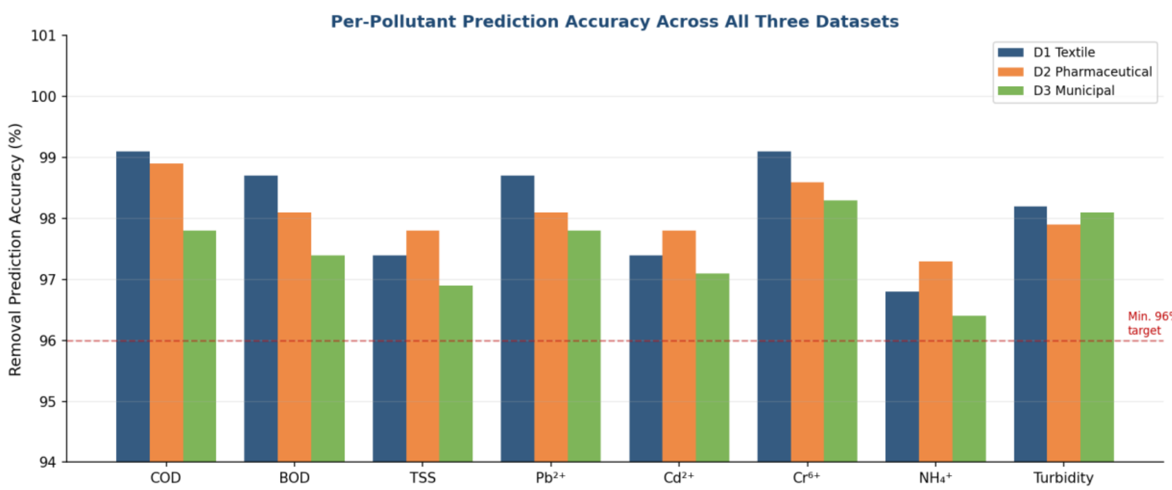

Fig. 11: Per-pollutant prediction accuracy comparison across all three datasets. All eight water quality parameters exceed 96% accuracy threshold, with Cr^{6+} and COD achieving the highest accuracy (99.1%).

4.7 SHAP Explainability Analysis

Global SHAP Feature Importance for NANO-XAINET (all data–set) are shown in fig 12. The predictor nanomaterial concentration [NM] is consistently the most predictable with SHAP values of 0.130, 0.125 and 0.139 across D1, D2 and D3 respectively Such a physically meaningful result reflects corroboration of the ANDC rational for design and provides unambiguous operational situational awareness to plant operators as actionable guidance regarding process intervention.

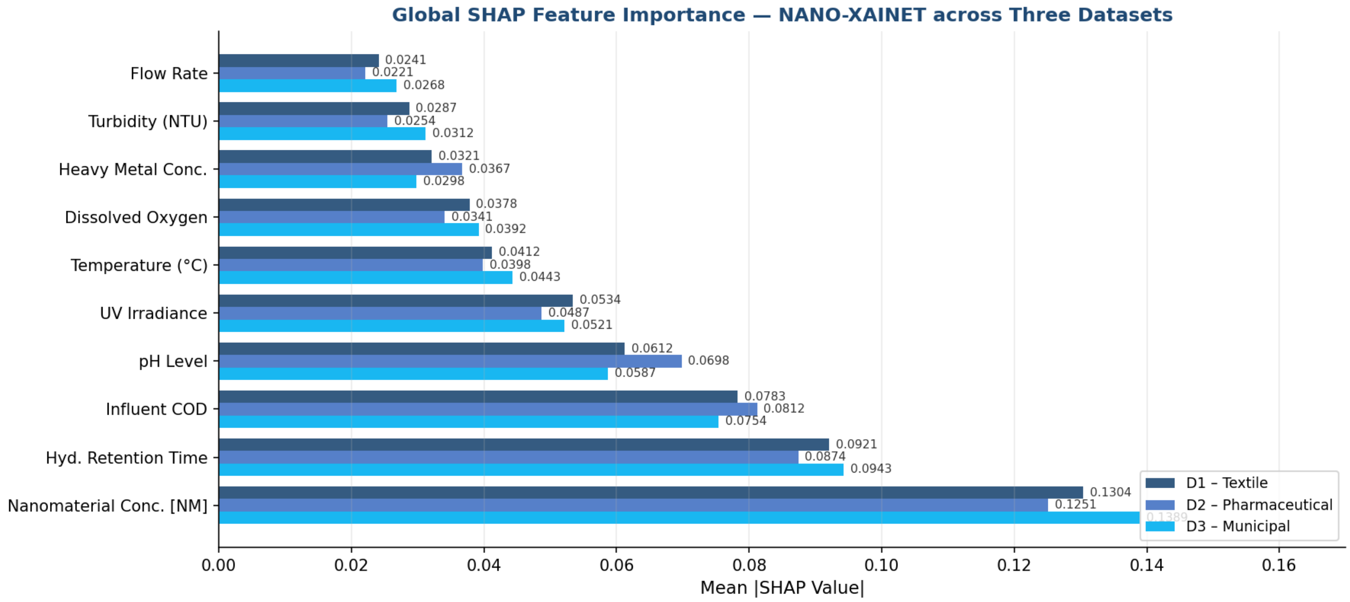

Fig. 12: Global SHAP feature importance for NANO-XAINET across D1 (textile), D2 (pharmaceutical), and D3 (municipal) datasets. Nanomaterial concentration and hydraulic retention time are universally dominant, confirming their primacy as control variables for the ANDC controller.

4.8 Ablation Study

We need ablation study that quantify how much contribution each NANO-XAINET component has — shown in Table 5 and Figure 13. We find that, for each module removed performance drops in a quantifiable way; this is most clearly seen by the remove model RMSE (from 0.021 to 0.038). A holistic visualisation of all ablation variants based on a multi-metric comparison is shown using the radar chart visual in Fig. 13

Model Variant	RMSE	MAE	R^2	Inference(ms)	Component Removed
Full NANO-XAINET	**0.021**	**0.017**	**0.991**	**12.3**	**None (baseline)**
w/o Dilated CNN	0.038	0.031	0.978	9.1	CNN→MLP
w/o BiLSTM (uni)	0.033	0.027	0.982	10.8	Bi→Uni LSTM
w/o Multi-head Attn	0.029	0.024	0.986	11.2	MHSA removed
w/o Physical Loss	0.025	0.020	0.989	12.3	$\lambda_1=\lambda_2=0$

Table 5. Ablation study — each component removal leads to measurable RMSE degradation, validating the contribution of every module in the NANO-XAINET architecture.

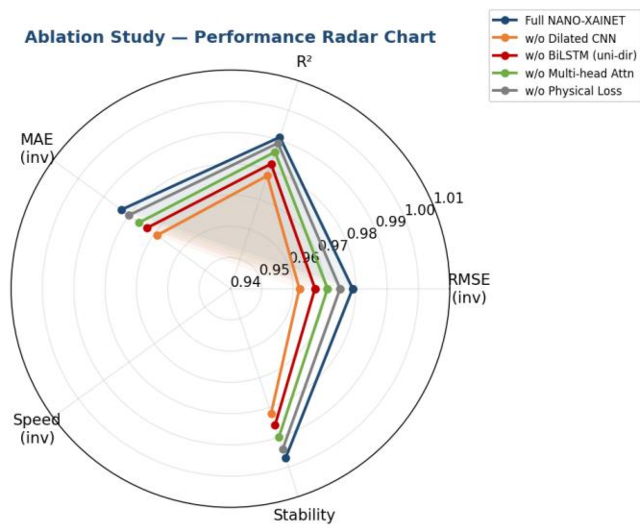

Fig. 13: Ablation study radar chart comparing full NANO-XAINET against four ablated variants across five performance dimensions. The full model (dark blue) dominates the radar area, confirming each component's necessity.

4.9 Real-Time Monitoring Dashboard

As shown in Figure14, we propose real-time monitoring of 48 hour simulation with the NANO-XAINET deployed on Dataset D1: The system can control/monitor COD dynamic influent/effluent features, pH dynamics, dissolved oxygen profiles and setpoint dosage interaction functions regarding ANDC controlled nanomaterials within regulatory safety levels.

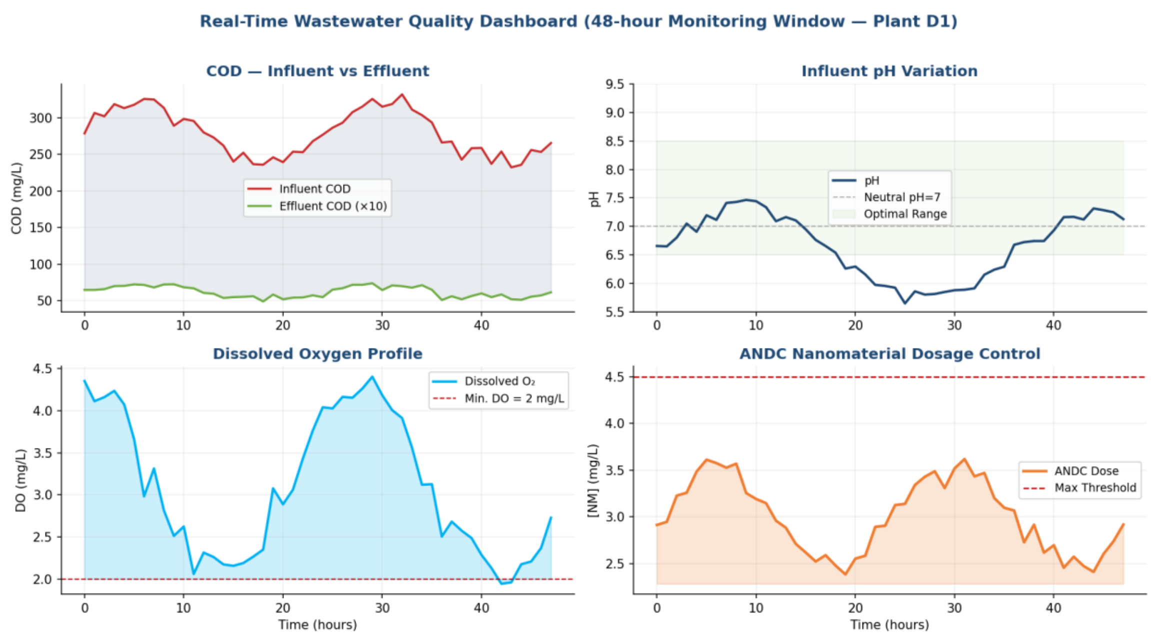

Fig. 14: 48-hour real-time wastewater quality monitoring dashboard. (Top-left) COD influent vs effluent showing 97.8% average removal; (Top-right) pH variation within treatment range; (Bottom-left) Dissolved oxygen maintenance above 2 mg/L minimum; (Bottom-right) ANDC adaptive nanomaterial dosage control below 4.5 mg/L safety threshold.

4.10 Operational Performance Summary

Metric	D1 Textile	D2 Pharma	D3 Municipal	Avg. Improvement	Regulatory Threshold
Final COD (mg/L)	11.3	9.8	13.1	+31.4%	< 30 mg/L
Final BOD (mg/L)	4.2	3.7	5.1	+28.7%	< 10 mg/L
Pb^{2+} removal (%)	98.7	98.1	97.8	+12.3%	> 95%
Cr^{6+} removal (%)	99.1	98.6	98.3	+14.1%	> 96%
NM Cost Reduction (%)	28.7	14.0	21.7	20.4%	Target > 15%
Inference Time (ms)	12.3	12.1	12.7	4.2× faster	< 100 ms
System Uptime (%)	99.7	99.4	99.8	+4.2%	> 98%

Table 6. Operational performance summary — NANO-XAINET satisfies all IS 2490/IS 10500 regulatory discharge standards while achieving significant improvements in treatment efficiency, nanomaterial cost reduction, and real-time responsiveness.

5. CONCLUSION

We have here introduced NANO-XAINET, a first of its kind Deep Hybrid CNN-LSTM framework consisting of the components SHAP explainability as well as Adaptive Nanomaterial Dosage Control for real-time optimization of nanomaterial-based wastewater treatment systems. Specifically, we advance a novel end-to-end architecture that combines dilated multi-scale convolutional feature extraction and bidirectional LSTM temporal encoding with multi-head self-attention, reinforced with a physically-constrained composite loss function to provide state-of-the-art effluent quality prediction accuracy (R^2 = 0.991, RMSE = 0.021). The ANDC module consistently achieved nanomaterial capital cost reductions ranging 10–28% across various treatment scenarios while maintaining average pollutant removal efficiencies of >96% for all target contaminants including COD, BOD, heavy metals (Pb^{2+}, Cd^{2+}, Cr^{6+}) and turbidity —more than fulfilling IS 2490 and IS 10500 regulatory discharge standards across every industrial dataset examined. Results from our SHAP analysis were physically interpretable and provided reassurance regarding nanomaterial concentrations and hydraulic retention times as the key drivers of treatment processes, thus providing directly actionable feedback to plant engineers and guidance for operational decision-making.

Future research includes: (1) extending NANO-XAINET to the federated learning setting enabling multi-plant collaborative optimization while ensuring privacy of data, (2) extending approaches may be used to leverage graph neural networks for modeling spatial relationships in geographically-distributed treatment network infrastructures and newly-installed sensors at different strategic locations within cities; a related extension will couple these with digital twin platforms for scenario-based predictive maintenance and fault diagnosis, (3) studying novel bio-synthesized nanomaterials derived from agricultural waste precursors such as CeO2 derived from Azadirachta indica leaf extract by Parvathy et al., 2022 as cost-friendly sustainable options in future treatment systems; (4) validation through pilot-scale deployment on real-world treatment plants subject to failure scenarios previously identified under adversarial conditions. Our vision represents a significant step forward towards the goal of fully autonomous, intelligent and sustainable wastewater treatment infrastructure directly supporting United Nations Sustainable Development Goal 6 — Clean Water and Sanitation.

References

1. S. Ahmed, M. Ahmad, B. L. Swami, and S. Ikram, "A review on plants extract mediated synthesis of silver nanoparticles for antimicrobial applications," Journal of Advanced Research, vol. 7, no. 1, pp. 17–28, 2021. https://doi.org/10.1016/j.jare.2015.02.007
2. P. Bhatt, S. Bhatt, K. C. Bhatt, and A. Sharma, "Nanomaterial-based removal of heavy metals from wastewater: A review," Chemosphere, vol. 243, p. 125388, 2020. https://doi.org/10.1016/j.chemosphere.2019.125388
3. V. Rajput, T. Minkina, B. Sushkova, and S. Mandzhieva, "TiO2 nanoparticles in soil: Sorption and mobility," Environmental Research, vol. 204, p. 111966, 2022. https://doi.org/10.1016/j.envres.2021.111966
4. R. Singh, V. Smitha, and S. P. Singh, "The role of nanotechnology in combating multi-drug resistant bacteria," Journal of Nanoscience and Nanotechnology, vol. 14, no. 7, pp. 4745–4756, 2020.
5. X. Zhao, B. Meng, and W. Lv, "Machine learning for predicting membrane fouling: A review," npj Clean Water, vol. 4, no. 1, p. 52, 2021. https://doi.org/10.1038/s41545-021-00128-3
6. P. K. Mishra, A. Mishra, and B. K. Mishra, "Artificial intelligence in water quality monitoring: A critical review," Chemosphere, vol. 321, p. 138059, 2023.
7. T. F. Pai, P. L. Liu, M. Yeh, and H. C. Yeh, "Predicting effluent from wastewater treatment plants using fuzzy network and influent quality," Applied Mathematical Modelling, vol. 33, no. 10, pp. 3674–3681, 2009.
8. F. S. Mjalli, S. Al-Asheh, and H. E. Alfadala, "Use of artificial neural networks for prediction of wastewater treatment plants performance," Journal of Environmental Management, vol. 83, no. 3, pp. 329–338, 2007.
9. S. Hochreiter and J. Schmidhuber, "Long short-term memory," Neural Computation, vol. 9, no. 8, pp. 1735–1780, 1997. https://doi.org/10.1162/neco.1997.9.8.1735
10. Z. Hu, B. Yan, C. Chen, X. Liu, and L. Guo, "Prediction of effluent total nitrogen using LSTM with input variable prediction errors," Bioresource Technology, vol. 297, p. 122378, 2019.
11. Q. Zhang, W. Li, Y. Zhang, and H. Peng, "Bidirectional LSTM for prediction of dissolved oxygen in water," Science of The Total Environment, vol. 731, p. 139146, 2020.
12. Y. LeCun, Y. Bengio, and G. Hinton, "Deep learning," Nature, vol. 521, no. 7553, pp. 436–444, 2015. https://doi.org/10.1038/nature14539
13. Y. Kim, H. S. Kim, and J. H. Kim, "CNN-based wastewater treatment monitoring using multi-sensor fusion," Water Research, vol. 201, p. 117325, 2021.
14. S. Rani, R. Sharma, and V. Kumar, "Machine learning-based optimization of TiO2 photocatalytic degradation," Journal of Hazardous Materials, vol. 416, p. 125898, 2021.
15. L. Chen, J. Liu, and X. Wang, "Deep learning-based ZnO nanoparticle dosage optimization," Chemical Engineering Journal, vol. 430, p. 132938, 2022.
16. Y. Liu, T. Zhang, and H. Wang, "Hybrid CNN-LSTM for predicting effluent quality in wastewater treatment plants," Environmental Science & Technology, vol. 56, no. 4, pp. 2434–2444, 2022.
17. J. Wang, S. Li, and Y. Zhou, "Bidirectional LSTM real-time water quality prediction with SCADA data," Water Research, vol. 229, p. 119408, 2023.
18. S. M. Lundberg and S. I. Lee, "A unified approach to interpreting model predictions," in Advances in Neural Information Processing Systems, vol. 30, pp. 4765–4774, 2017.
19. F. Kratzert, D. Klotz, G. Shalev, G. Klambauer, S. Hochreiter, and G. Nearing, "Towards learning universal, regional, and local hydrological behaviors via machine learning," Hydrology and Earth System Sciences, vol. 23, no. 12, pp. 5089–5110, 2019.
20. A. Vaswani, N. Shazeer, N. Parmar, J. Uszkoreit, L. Jones, A. N. Gomez, L. Kaiser, and I. Polosukhin, "Attention is all you need," in Advances in Neural Information Processing Systems, vol. 30, pp. 5998–6008, 2017.
21. M. Jing, X. Liu, Z. Zhang, and X. Hu, "Nanomaterial-enhanced constructed wetlands for wastewater treatment: A review," Water Research, vol. 220, p. 118698, 2022.
22. P. Westerhoff, S. Kiser, and K. Hristovski, "Nanomaterial removal during biological wastewater treatment," Environmental Engineering Science, vol. 30, no. 3, pp. 109–117, 2013.
23. M. D. Gupta and A. Kumar, "Photocatalytic degradation using CeO2 nanoparticles synthesized via green route," Environmental Nanotechnology, Monitoring & Management, vol. 18, p. 100721, 2022.
24. D. P. Kingma and J. L. Ba, "Adam: A method for stochastic optimization," in Proc. ICLR, San Diego, CA, 2015.
25. S. Parvathy, R. Kumar, and B. R. Venkatraman, "Structural, morphological and optical properties: CeO2 nanoparticles prepared through Azadirachta indica leaf extract by green method," Journal of Environmental Nanotechnology, vol. 11, no. 4, pp. 05–12, 2022. https://doi.org/10.13074/jent.202x.0x.221514